# Supplementary Information for
# Ambipolar device simulation based on the drift-diffusion model in ion-gated transition metal dichalcogenide transistors

Akiko Ueda,[1,2] Yijin Zhang,[3,4] Nobuyuki Sano,[5] Hiroshi Imamura,[1] and Yoshihiro Iwasa[6,7]

[1]*National Institute of Advanced Industrial Science and Technology (AIST) ,*
*Spintronics Research Center, Tsukuba, 305-8568, Japan*

[2]*Department of Electrical Engineering,*
*Columbia University, New York, NY, USA*

[3]*The Institute of Scientific and Industrial Research,*
*Osaka University, Osaka, 067-0047, Japan*

[4]*Max Planck Institute for Solid State Research, Stuttgart, D-70569, Germany*

[5]*Institute of Applied Physics, University of Tsukuba, Tsukuba, 305-8573, Japan*

[6] *Department of Applied Physics and Quantum-Phase Electronics (QPEC) Center,*
*The University of Tokyo, Tokyo, 113-8656, Japan*

[7]*RIKEN, Center for Emergent Matter Science (CEMS), Wako, 351-0198, Japan*

## I. SCHARFETTER-GUMMEL DISCRETIZATION

For the numerical calculation, we use the Scharfetter-Gummel discretization to solve the DD equation which is modified under the generalized Einstein relation. The Scharfetter-Gummel discretization is adopte for the unified mesh since it is suitable to determine carrier concentration whose change is precipitous. Assuming that $\nabla\Phi$ and $J_{\mathrm{n(p)}}$ are constant between the meshes $x_i$ and $x_{i+1}$, the current densities for electrons and holes are written as

$$
\begin{aligned}
J_{\mathrm{n}}(x_{i+1/2}) &= -q\mu_{\mathrm{e}}\frac{\Phi(x_{i+1},0)-\Phi(x_i,0)}{dx}\frac{n(x_{i+1})-\exp\left\{\frac{\Phi(x_{i+1},0)-\Phi(x_i,0)}{V_{\mathrm{T}}\sqrt{g_{\mathrm{n}}(x_i)g_{\mathrm{n}}(x_{i+1})}}\right\}n(x_i)}{1-\exp\left\{\frac{\Phi(x_{i+1},0)-\Phi(x_i,0)]}{V_{\mathrm{T}}\sqrt{g_{\mathrm{e}}(x_i)g_{\mathrm{n}}(x_{i+1})}}\right\}}, &(1)\\
J_{\mathrm{p}}(x_{i+1/2}) &= -q\mu_{\mathrm{h}}\frac{\Phi(x_{i+1},0)-\Phi(x_i,0)}{dx}\frac{p(x_i)-\exp\left\{\frac{\Phi(x_{i+1},0)-\Phi(x_i,0)}{V_{\mathrm{T}}\sqrt{g_{\mathrm{h}}(x_i)g_{\mathrm{h}}(x_{i+1})}}\right\}p(x_{i+1})}{1-\exp\left\{\frac{\Phi(x_{i+1},0)-\Phi(x_i,0)}{V_{\mathrm{T}}\sqrt{g_{\mathrm{p}}(x_i)g_{\mathrm{p}}(x_{i+1})}}\right\}}, &(2)
\end{aligned}
$$

where $V_{\mathrm{T}} = k_{\mathrm{B}}T/q$. Then, the contituity equations for electrons and holes are written as

$$
\begin{aligned}
\frac{J_{\mathrm{n}}(x_{i+1/2}) - J_{\mathrm{n}}(x_{i-1/2})}{x_{i+1} - x_i} &= qR(x_i),\\
\frac{J_{\mathrm{p}}(x_{i+1/2}) - J_{\mathrm{p}}(x_{i-1/2})}{x_{i+1} - x_i} &= -qR(x_i). &(3)
\end{aligned}
$$

Here, we determine the carrier concentration $n(x_i)$ and $p(x_i)$ using the continuity equation. Note that for the carrier with the Boltzmann distribution, $g_{\mathrm{n(p)}}(x_i) = 1$.

## II. RECOMBINATION RATE OF ELECTRONS AND HOLES IN AMBIPOLAR REGION

In Supplementary Figure 1, we plot the recombination rate of the direct recombination, $R_{\rm dir}$, and the SRH recombination $R_{\rm SRH}$ as a function of the location $x$ in the saturation region, $V_{\rm ds} = 2.5$V, and the ambipolar region, $V_{\rm ds} = 4$V. Note that $R_{\rm dir}$ and $R_{\rm SRH}$ are zero for $V_{\rm ds} = 0.5$V, since the $p(x) = 0$ in the linear region. As shown from the figure, the electron-hole recombination is yielded in the whole channel area since the size of the recombination zone is about 1 $\mu$m which is much larger than the channel size $L_x$ considered in this paper.

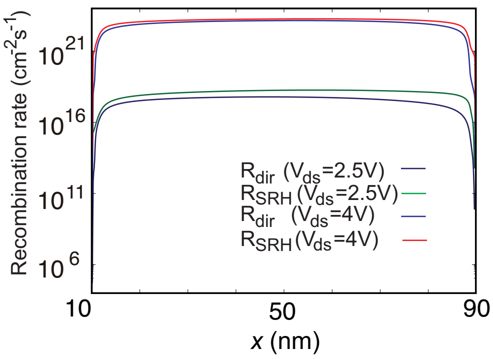


Supplementary Figure 1: Recombination rate for the direct recombination and the SRH recombination for $V_{\rm ds} = 2.5$V and $V_{\rm ds} = 4$V.

## III. WSE$_2$ MOS TRANSISTORS

In this section, we calculate the $WSe_2$ transistor with the same structure as Fig. 1, but the IL is replaced with the oxide layer as shown in Supplementary Fig. 2a. Note that in experiments, the conventional $WSe_2$ metal-oxide-semiconductor (MOS) transistors are usually p-type due to unintentional doping. However, we adopt the intrinsic $WSe_2$ with the n-type contact to compare the results with the ion-gating $WSe_2$ transistors. The gate voltage is fixed to 10 V. The carrier concentration for the gate voltage is approximately 5 $\times 10^{13}$ cm$^{-2}$. The oxide layer has same relative permittivity ($\epsilon_{\rm ox} = 10$) with the one for IL. In Supplementary Fig. 2b, we plot the current as a function of $V_{\rm ds}$. The current is almost linearly increasing since the threshold voltage and the pinch-off voltage for $V_{\rm gs} = 10$V is much larger than $V_{\rm ds} = 4$ V. Supplementary Figure 3 shows the band profile of $WSe_2$ for $V_{\rm ds} = 0.5$V, 2.5V, and 4V. For $V_{\rm ds} = 2.5$V, and 4V, the potential drops mainly at the source region and also decreases at the channel linearly. At the drain region, the

Schottky barrier does not prevent electrons pass through the $WSe_2$-metal junction and acts as the perfect Ohmic contact. Since the Fermi energy of the metal contact is located inside the band gap, holes at the drain contact cannot pass through the junction. Thus, the MOS transistor is n-type up to $V_{\rm ds} = 4$V.

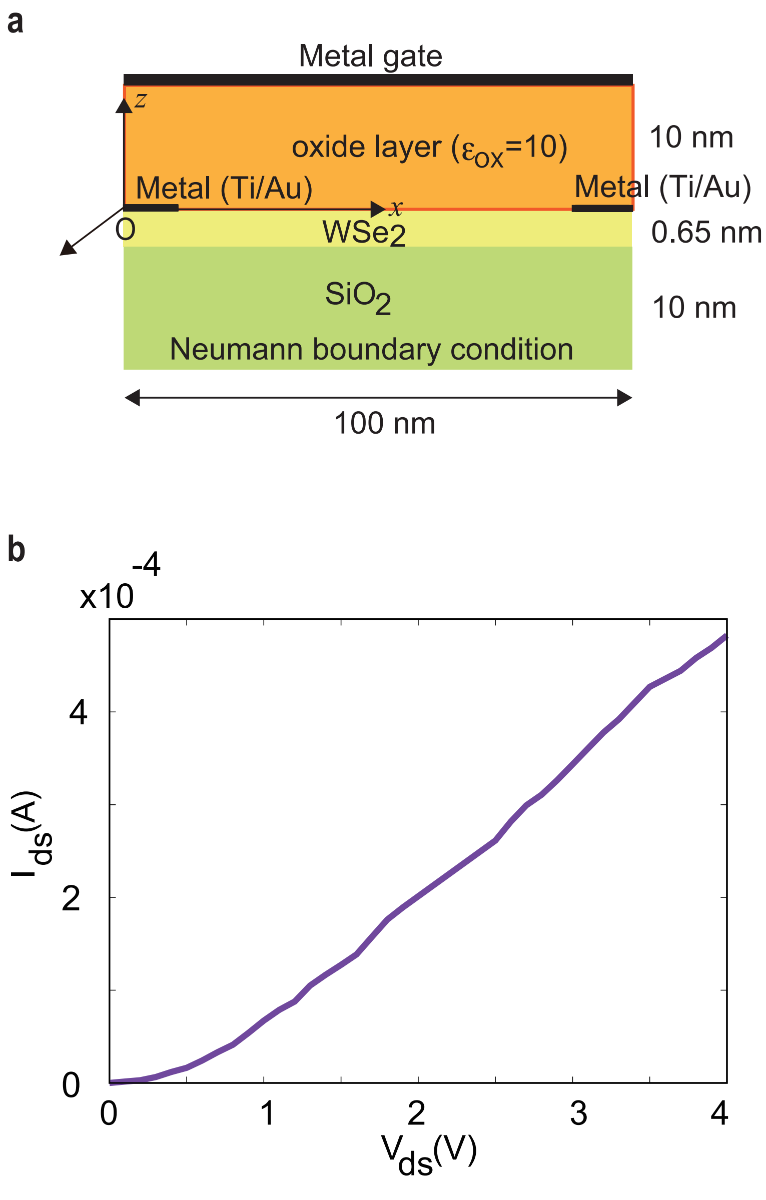


Supplementary Figure 2: **a** Model of MOS transistors. **b** The current for the MOS transistor at $V_{\rm gs} = 10$V.

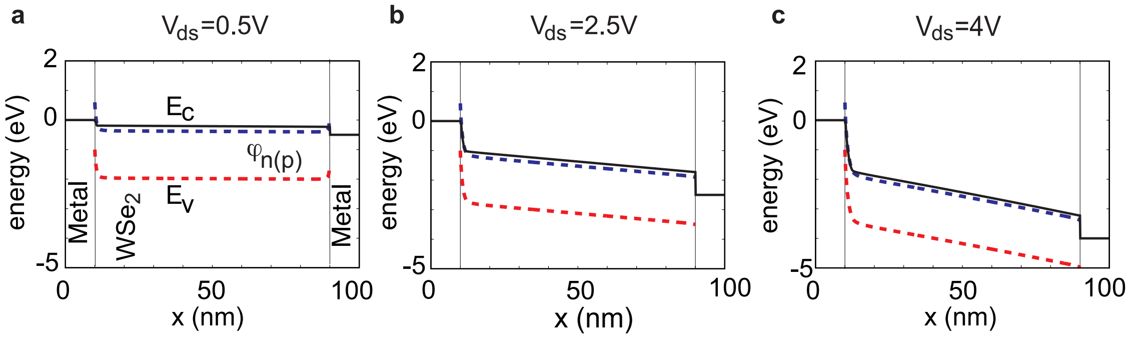


Supplementary Figure 3: The band profile of **a** $V_{\rm ds} = 0.5$V, **b** $V_{\rm ds} = 2.5$V and **c** $V_{\rm ds} = 4$V for the $WSe_2$ MOS transistors.